



저작자표시-비영리-변경금지 2.0 대한민국

이용자는 아래의 조건을 따르는 경우에 한하여 자유롭게

- 이 저작물을 복제, 배포, 전송, 전시, 공연 및 방송할 수 있습니다.

다음과 같은 조건을 따라야 합니다:



저작자표시. 귀하는 원저작자를 표시하여야 합니다.



비영리. 귀하는 이 저작물을 영리 목적으로 이용할 수 없습니다.



변경금지. 귀하는 이 저작물을 개작, 변형 또는 가공할 수 없습니다.

- 귀하는, 이 저작물의 재이용이나 배포의 경우, 이 저작물에 적용된 이용허락조건을 명확하게 나타내어야 합니다.
- 저작권자로부터 별도의 허가를 받으면 이러한 조건들은 적용되지 않습니다.

저작권법에 따른 이용자의 권리는 위의 내용에 의하여 영향을 받지 않습니다.

이것은 [이용허락규약\(Legal Code\)](#)을 이해하기 쉽게 요약한 것입니다.

[Disclaimer](#)

Modified Dixon fat-water imaging for
detecting intravertebral fracture line in
the benign and malignant vertebral
compression fractures : usefulness of
fat, water, in phase and opposed phase
imaging

Bo Yeon Kim

Department of Medicine

The Graduate School, Yonsei University

Modified Dixon fat-water imaging for
detecting intravertebral fracture line in
the benign and malignant vertebral
compression fractures : usefulness of
fat, water, in phase and opposed phase
imaging

Bo Yeon Kim

Department of Medicine

The Graduate School, Yonsei University

Modified Dixon fat-water imaging for
detecting intravertebral fracture line in
the benign and malignant vertebral
compression fractures : usefulness of
fat, water, in phase and opposed phase
imaging

Directed by Professor Jin-Suck Suh

The Master's Thesis submitted to the Department of
Medicine, the Graduate School of Yonsei University
in partial fulfillment of the requirements for the degree
of Master of Medical Science

Bo Yeon Kim

June 2018

This certifies that the Master's Thesis of
Bo Yeon Kim is approved.

Thesis Supervisor : Jin-Suck Suh

Thesis Committee Member#1 : Young Han Lee

Thesis Committee Member#2 : Do Sik Hwang

The Graduate School
Yonsei University

June 2018

ACKNOWLEDGEMENTS

I would like to express my sincere gratitude to Professor Jin-Suck Suh and Young Han Lee for his generous support and encouragement for this research and to Professor Do Sik Hwang for his advice to supplement this research.

In addition, I would like to express my sincere gratitude to Dr. Seung Hyun Lee for helping me as a co-worker during my dissertation research and to my beloved family.

<TABLE OF CONTENTS>

ABSTRACT	1
I. INTRODUCTION	3
II. MATERIALS AND METHODS	4
1. Patients	4
2. Imaging protocol	5
3. Imaging analysis	6
4. Statistical analysis	8
III. RESULTS	8
1. Patients demographics	8
2. Comparison of the diagnostic performance	9
IV. DISCUSSION	13
V. CONCLUSION	17
REFERENCES	18
ABSTRACT (IN KOREAN)	20

LIST OF FIGURES

Figure 1. Example for what we determined as fracture line.	6
Figure 2. Example for what we did not determine as fracture line.	7
Figure 3. Comparison of the sensitivity of IP images, WO images, FO images, and OP images of modified Dixon MRI technique.	11
Figure 4. Illustration of the specificity of IP images, WO images, FO images, and OP images of mDixon MRI technique.	12
Figure 5. Successful detection of intravertebral fracture line using mDixon MRI technique only at OP image.	14
Figure 6. Successful detection of intravertebral fracture line using mDixon MRI technique except for FO image.	16

LIST OF TABLES

Table 1. The diagnostic performance of mDixon MRI findings of the fracture line	10
Table 2. Statistical significance using Bonferroni correction method	10
Table 3. Interobserver reliability using Kappa	12

ABSTRACT

Modified Dixon fat-water imaging for detecting intravertebral fracture line in the benign and malignant vertebral compression fractures : usefulness of fat, water, in phase and opposed phase imaging

*Department of Medicine
The Graduate School, Yonsei University*

(Directed by Professor Jin-Suck Suh)

The purpose of this study is to evaluate the diagnostic role of the modified Dixon magnetic resonance imaging for differentiation between benign vertebral compression fractures and malignant vertebral compression fractures focusing on the intravertebral fracture line.

Patients were initially enrolled from April 2014 to August 2016. Sixty patients with a radiological report of vertebral compression fractures were collected. All sixty patients underwent sagittal T2-weighted two-point modified Dixon turbo spin echo sequences. After application of the exclusion criteria, 37 patients were finally enrolled. The clinical history, pathologic confirmation, and positron emission tomography-computed tomography within 5 months from the time of modified Dixon magnetic resonance imaging examination were used as a reference standard to differentiate between benign vertebral compression fractures and malignant vertebral compression fractures. Two radiologists independently evaluated the presence or absence of the fracture lines on sagittal T2-weighted two-point modified Dixon turbo spin echo sequences. Sensitivities, specificities, positive predictive values, negative predictive values, and accuracies in detecting fracture line on water only image, fat only image, in phase image, and opposed phase image were determined with the generalized

estimating equation method or weighted least square. The interobserver reliability was evaluated by kappa value.

A total of 73 vertebral body collapse were found in 37 patients : study group was composed of 14 patients with 32 benign vertebral compression fractures and 23 patients with 41 malignant vertebral fractures. The sensitivity of opposed phase image was higher than that of water only image, fat only image, and in phase image in the post hoc Bonferroni test with $p < 0.05$. The specificity of fat only image was higher than that of water only image, in phase image, and opposed phase image ($p < 0.0001$). The positive predictive value of fat only image was significantly higher than that of water only image, in phase image, and opposed phase image (p value less than 0.05). Interobserver reliability was substantial to good.

In conclusion, modified Dixon magnetic resonance imaging may be a helpful option in patients to discriminate benign vertebral compression fractures and malignant vertebral compression fractures.

Key words : modified Dixon magnetic resonance imaging, benign, malignant, vertebral compression fracture, fracture line

Modified Dixon fat-water imaging for detecting intravertebral fracture
line in the benign and malignant vertebral compression fractures :
usefulness of fat, water, in-phase and opposed-phase imaging

Department of Medicine
The Graduate School, Yonsei University

(Directed by Professor Jin-Suck Suh)

I. INTRODUCTION

Two-point Dixon methods rely on the phase shifts created by fat-water resonance frequency differences to separate water from fat. Phase information is encoded by acquiring images at slightly different echo times (TE), exploiting the difference in resonance frequency between water and fat. Water and fat were “in phase (IP)” [$S_{in} = W+F$] or “opposed phase (OP)” [$S_{opp} = W-F$]. By adding and subtracting S_{in} and S_{opp} , water-only (WO) and fat-only (FO) images are easily separated, since $WO = [S_{in} + S_{opp}]/2$, and $FO = [S_{in} - S_{opp}]/2$.¹ Recent advances in the Dixon technique have led to the development of a new two-point Dixon method, the modified Dixon (mDixon), with flexible choice of TE for water-fat separation, using the referenced seven-peak spectral model of fat in the separation². The mDixon technique automatically calculates the two shortest TEs, which allows an improved signal to noise ratio while maintaining high spatial resolution.²

Among the four phases of mDixon technique (WO, FO, IP, OP sequence), the india ink artifact can be recognized as a characteristic sharp black line at fat-water (fat-muscle or fat-solid organ) interfaces on OP image. It is due to the presence of fat and water protons within the same imaging voxel, resulting in signal loss³ It occurs along the entire border of fat-water interfaces and not only in the frequency-encoding direction because it is a result of fat and water proton phase cancellation in all directions⁴

Recently, several studies regarded mDixon MRI or opposed phase

technique representing india-ink artifact as an helpful option to improve the diagnostic performance in the field of abdominal imaging and musculoskeletal radiology.

Israel et al revealed the presence of india artifact at a renal mass-kidney interface or within a renal mass is indicative of angiomyolipoma on opposed phase chemical shift MRI.⁵ Likewise, Park et al reported a case of nondisplaced chip fracture at the lateral talar dome that was well delineated only with the aid of a india ink artifact, which was visualized using T2-weighted opposed phase imaging from turbo spin-echo (TSE) two-point mDixon MRI.⁶

Based on the related papers mentioned above, we assumed that mDixon MRI also might be an effective tool to differentiate benign vertebral compression fracture(VCF) and malignant VCF by helping to detect the benign vertebral compression fracture line which might be depicted as india-ink artifact on OP image. Unlike benign VCF, malignant VCF can occur due to entire neoplastic infiltration, resulting in the loss of intravertebral fracture line. This is the reason why presence of fracture line is highly suggestive of benign rather than malignant.⁷ Also, we investigated whether the other mDixon MRI sequences had a diagnostic role in detecting fracture line. Good depiction of the fracture line using mDixon MRI will help radiologist to distinguish benign from malignant, which could result in increase of diagnostic performance.

The purpose of this study was to determine the reliability of the mDixon MRI to differentiate benign VCFs from pathologic VCFs focusing on the intravertebral fracture line.

II. MATERIALS AND METHODS

Patients

The institutional review board approved this study and informed consent was waived due to the retrospective nature of the study. Patients were initially enrolled from April 2014 to August 2016. Sixty patients with a radiological

report of VCF were collected. All sixty patients underwent sagittal T2-weighted two-point mDixon TSE sequences. Among these, 23 patients were excluded due to (a) pathologic VCFs without PET-CT within 5 months from the time of mDixon magnetic resonance imaging (MRI) examination or without bone biopsy result (n=13), (b) old VCFs (n=4), (c) uncertain diagnosis after positron emission tomography-computed tomography (PET-CT) (n=2), (d) previous vertebroplasty (n=2), (e) diagnostic difference between PET-CT and bone biopsy (n=1), (f) diagnostic difference between PET-CT and MRI (n=1). The remaining 37 patients were finally included in the present study. Diagnosis of a benign VCF was made on the basis of medical history, PET-CT, and bone biopsy. The diagnosis of benign VCF was classified as follows : (a) trauma history without known history of malignancy, (b) diagnosis of benign VCF after PET-CT despite known history of malignancy. The diagnosis of malignant VCF was made based on (a) the presence of a malignant tumor from the bone biopsy specimen, (b) a radiological report of pathologic VCF on PET-CT within 5 months from the time of mDixon MRI examination with known history of malignancy.

Imaging protocol

All thoracic spine, lumbar spine, and whole spine MRI were performed with a 3.0 Tesla MRI scanner (Ingenia, Philips Healthcare, Best, Netherlands) using the two-point mDixon TSE technique with flexible TEs and multipeak spectral model of fat. MRIs had been acquired with patients in the supine position using the built-in posterior coil and the base coil (44-channel array, Philips Healthcare, Best, Netherlands). A sagittal T2-weighted two-point mDixon TSE sequence had been used in addition to routine sequences including sagittal T1-weighted, axial T2-weighted, axial T1-weighted, and whole spine sagittal T2-weighted images. Sagittal T2-weighted mDixon images were automatically reconstructed into WO images, FO images, IP images, and OP images by the fat-water separation algorithm in one acquisition requiring no additional scans, that is, without increasing scan time.⁸ Imaging parameters were performed as follows; field of

view, 240-380 mm for the sagittal plane; matrix size, 400-512 x 183-352 mm; section thickness/intersection gap, 3 mm/0.3mm or 4mm/0.4mm; repetition time, 2000-3000; TE, 80-120; flip angle, 90 degrees; number of excitations, 1; echo train length, 21-30.

Imaging analysis

All MR imaging were reviewed by two musculoskeletal radiologists (B. Y. Kim, with 1 year of experience; and S. H. Lee, with 2 years of experience) independently, who were blind to the clinical data. Two observers independently evaluated the presence or absence of the fracture lines on sagittal T2-weighted two-point mDixon TSE sequence after previewing five cases with senior radiologist (Y. H. Lee, with more than 10 year of experience) how fracture lines would be determined. Window level was adjusted respectively optimized for evaluation.

Bandlike low signal intensity corresponding to the fracture site is exclusively determined as fracture line (Figure 1.). We carefully judged not to determine the shadow due to basivertebral vein as fracture line.



Figure 1. Benign multilevel VCF appeared after trauma in a 41-year old woman who had past history adrenocortical carcinoma. Low signal intensity bands (arrow) were depicted along multilevel thoracic vertebrae on sagittal T2-

weighted WO (a), FO (b), IP (c), OP (d) MR images (TR/TE, 2300/100) resulting from axial loading. India ink artifact shown on OP image highlights contrast between fracture line and fatty marrow.

The line along the entire boundary of the malignant mass is not determined as fracture line (Figure 2.). Any discrepancy between two radiologists is settled by consensus.

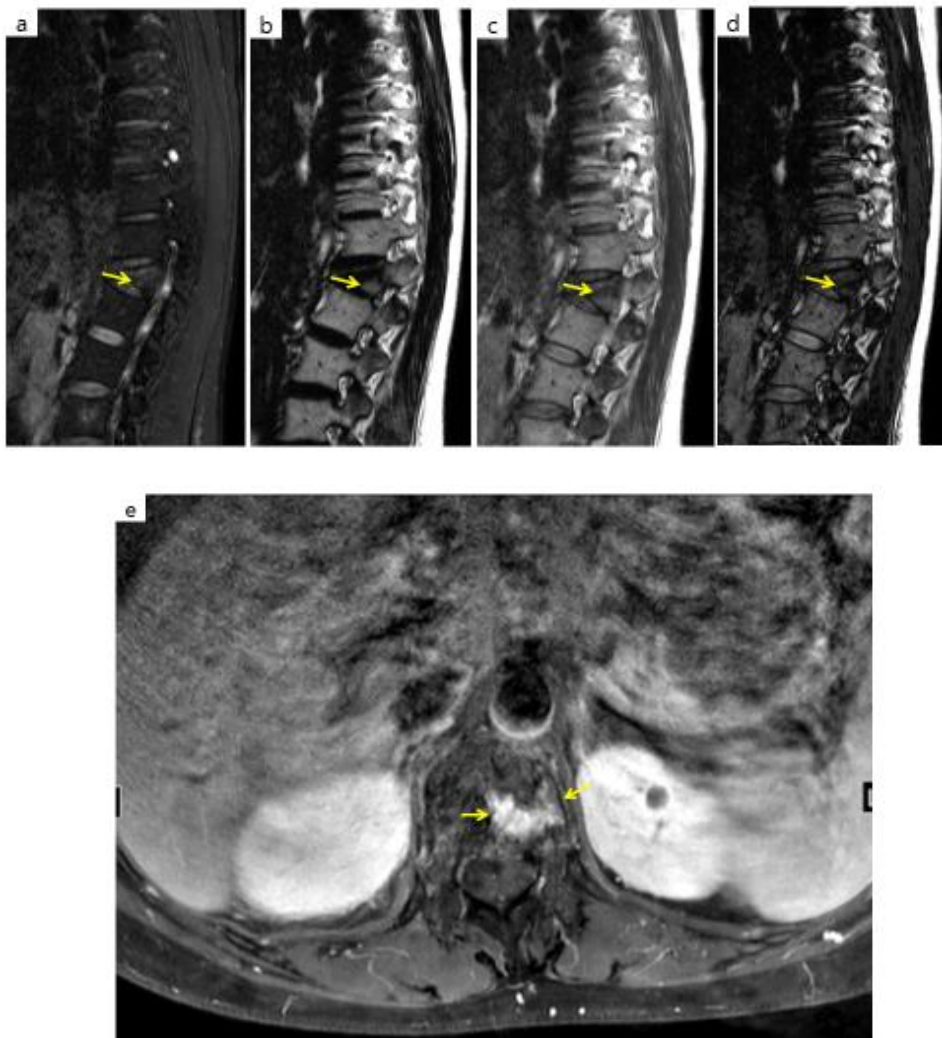


Figure 2. Malignant VCF of T12 vertebral body in a 52-year old woman without known history of multiple myeloma. Note the black line along the interface of the multiple myeloma with fatty marrow (arrow) on sagittal T2-weighted WO (a), FO (b), IP (c), OP (d) MR images (TR/TE, 2500/100), which is excluded from fracture line. Multiple myeloma is confirmed through contrast enhanced T1-weighted image (e) (arrow) (TR/TE, 561.864/15), where we could find the enhancing mass in the left side of T12 vertebral body.

Statistical analysis

We calculated and compared the sensitivity, specificity, positive predictive value, negative predictive value, and accuracy in detecting fracture line on WO images, FO images, IP images, and OP images, for each observer, with the generalized estimating equation method. However, if there are 0 cells in true positive, true negative, false positive, and false negative, we compare the two methods by weighted least square method. Analysis was performed using SAS Version 9.4(SAS Institute, Cary, NC, U.S.A). The Bonferroni correction method was used, and statistical significance was assumed when the p value was ,0.05. Interobserver reliability was assessed by kappa value in each finding and was classified as follows; poor, 0-0.20; fair, 0.21-0.40; moderate, 0.41-0.60; substantial, 0.61-0.80; and good, 0.81-1.00.

III. RESULTS

Patients demographics

A total of 73 vertebral body collapse were found in 37 patients : 23 patients with single level lesion and 14 patients with multiple levels of lesions. In the benign VCFs, there were one patient with seven-level fractures, one patient with five-level fractures, one patient with four-level fractures, two patients with three-level fractures, and one patient with two-level fractures. In the malignant VCFs, three patients with three-level fractures, three patient with two-level fractures, one patient with seven-level fractures, and one patient with four-level fractures.

Biopsy and PET-CT were not performed in 4 patients because of apparent history of trauma without known history of malignancy. Surgical biopsy was performed in 1 patient (malignant peripheral nerve sheath tumor). 32 patients with known history of malignancy underwent PET-CT within 5 months from the time of mDixon MRI examination. VCFs were principally located in the thoracic spine (43/73), lumbar spine (19/73), and cervical spine (11/73). There were 18 men and 19 women with range of age of 23-83 years old; mean age 61.65 years old. In the benign VCFs, a total of 32 vertebral body collapse were found in 14 patients. In the malignant VCFs, a total of 41 vertebral body collapse were found in 23 patients. Primary malignancies in the group of benign VCFs included lung cancer (n=2), adrenocortical carcinoma (n=1), esophageal cancer (n=1), hepatocellular carcinoma (n=1), Hodgkin's disease (n=1), multiple myeloma (n=1), pancreatic cancer (n=1), prostate cancer (n=1), and malignant peripheral nerve sheath tumor (n=1). Primary malignancies in the group of malignant VCFs included breast cancer (n=6), lung cancer (n=5), multiple myeloma (n=4), rectal cancer (n=2), diffuse large B cell lymphoma (n=1), esophageal cancer (n=1), prostate cancer (n=1), sarcomatoid urothelial carcinoma (n=1), stomach cancer (n=1), and transitional cell cancer (n=1).

Comparison of the diagnostic performance

Table 1. summarizes the sensitivity, specificity, positive predictive value, and negative predictive value in the detection of fracture line. The sensitivity of WO images, FO images, IP images, and OP images was 59.38%, 53.13%, 75%, and 93.75%, respectively. The specificity of WO images, FO images, IP images, and OP images was 65.85%, 95.12%, 65.85%, and 63.42%, respectively. The sensitivity of OP images was higher than that of WO images, FO images, and IP images in the post hoc Bonferroni test with $p < 0.05$. The fact that the sensitivity of OP image is significantly higher than that of the FO image (similar character to a conventional T1-weighted image) and IP image (similar to a conventional T2-weighted image) is impressive in that it means OP image is

superior to the existing method in depiction of intravertebral fracture line. The specificity of FO images was higher than that of WO images, IP images, and OP images ($p < 0.0001$). The positive predictive value of FO images was significantly higher than that of WO images, IP images (again, similar to conventional T2-weighted image), and OP images ($p < 0.05$). The negative predictive value of OP images was significantly higher than that of FO images ($p = 0.004$).

Table 1. The diagnostic performance of mDixon MRI findings of the fracture line

	Sensitivity	Specificity	PPV	NPV	Accuracy
WO	59.38 (42.36- 76.39)	65.85 (51.34- 80.37)	57.58 (40.71- 74.44)	67.5 (52.99- 82.02)	63.01 (51.94- 74.09)
FO	53.13 (35.84- 70.42)	95.12 (88.53- 99.99)	89.47 (75.67- 99.99)	72.22 (60.28- 84.17)	76.71 (67.02- 86.41)
IP	75 (60.00- 90.00)	65.85 (51.34- 80.37)	63.16 (47.82- 78.50)	77.14 (63.23- 91.06)	69.86 (59.34- 80.39)
OP	93.75 (85.36- 99.99)	63.42 (48.67- 78.16)	66.67 (52.89- 80.44)	92.86 (83.32- 99.99)	76.71 (67.02- 86.41)

¹The value in parentheses is 95% confidence interval.

²PPV: positive predictive value, NPV: negative predictive value, WO: water only, FO: fat only, IP: in phase, OP: opposed phase.

Table 2. lists the p-values for comparison. OP images were of significant value in detection of fracture lines.

Table 2. Statistical significance using Bonferroni correction method.

	Sensitivity	Specificity	PPV	NPV	Accuracy
WO vs. FO	>.9999	<.0001*	0.0018*	>.9999	0.3702

WO vs. IP	>.9999	>.9999	>.9999	>.9999	>.9999
WO vs. OP	0.015*	>.9999	0.3738	0.255	0.4866
FO vs. IP	0.1374	<.0001*	0.0054*	>.9999	>.9999
FO vs. OP	<.0001*	<.0001*	0.015*	0.0036*	>.9999
IP vs. OP	0.0396*	>.9999	>.9999	0.054	0.3162

¹Bold font* means statistically significant.

²WO: water only, FO: fat only, IP: in phase, OP: opposed phase.

Figure 3. make it easier to figure out the sensitivity of the contents of the Table 1. Similarly, Figure 4. helps to comprehend the specificity of the contents of the Table 1.

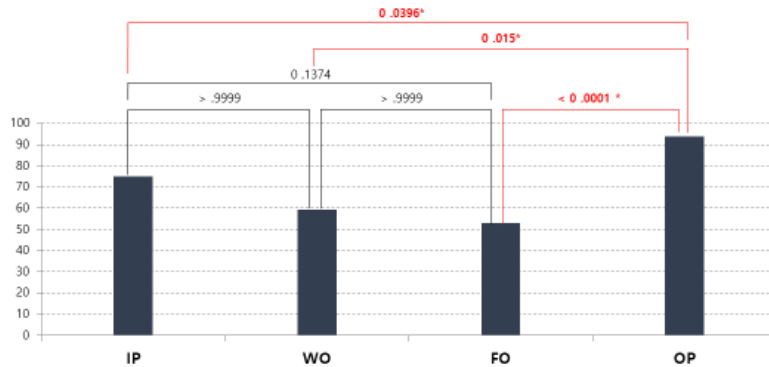


Figure 3. Comparison of the sensitivity of IP images, WO images, FO images, and OP images of mDixon MRI technique. OP images show statistically significant higher sensitivity compared to the other images. The values between the bars of a histogram mean the p values using Bonferroni correction method which indicate the statistical differences between each other. Bold font* means statistically significant.

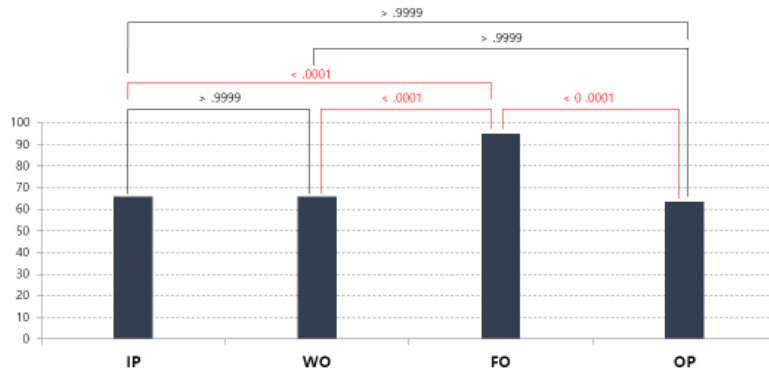


Figure 4. Illustration of the specificity of IP images, WO images, FO images, and OP images of mDixon MRI technique. FO images show statistically significant higher specificity compared to the other images. The values between the bars of a histogram mean the p values using Bonferroni correction method which indicate the statistical differences between each other. Bold font* means statistically significant.

The results of the interobserver reliability analysis are shown in Table 3. Interobserver reliability for WO images, FO images, and OP images was substantial ($0.6 < k \leq 0.8$) and reliability for IP was good ($k=0.8314$).

Table 3. Interobserver reliability using Kappa

	kappa	95% CI
WO	0.7222	(0.5627-0.8817)
FO	0.7321	(0.5596-0.9046)
IP	0.8314	(0.7024-0.9603)
OP	0.7099	(0.5458-0.8740)

¹CI: confidence interval, WO: water only, FO: fat only, IP: in phase, OP: opposed phase.

IV. DISCUSSION

There have been studies to differentiate benign VCF from malignant VCF based on recent MRI technique. First, Erly et al found that discrimination based on the signal intensity ratio of opposed phase/in phase was useful for differential diagnosis between malignant and benign VCFs.⁹ Likewise, the Dixon method allows for the direct quantification of the fat fraction in an area of interest, and can be used to look for replacement of normal fatty marrow by a tumor.^{8,10} Second, the role of diffusion-weighted images has been reported as an additional differentiation technique. Diffusion is presumed to be increased in osteoporotic fractures due to bone marrow edema, which allows relatively unimpeded extracellular water molecule movement.¹¹ With malignant VCF, diffusion is predicted to be restricted due to the typically high cellularity of tumor tissue.¹¹ However, to our knowledge, no studies have been published to use mDixon MRI to differentiate benign VCFs from malignant VCFs focusing on the intravertebral fracture line. The present study identified the reliability of mDixon MRI sequences to improve detection of fracture line.

Bone marrow is a complex heterogeneous admixture of hematopoietic red marrow and fatty yellow marrow supported by varying proportions of structural trabecular bone.¹² Benign VCFs frequently show normal marrow preservation with low signal intensity band corresponding to impacted, fractured bone or necrotic portions, which interfere with medullary water-fat balance.^{7,12}

OP images have well-documented noncontrast imaging benefits, as normal background fat and water marrow signals cancel serving to highlight marrow infiltrating pathology.¹³ An india ink artifact would be seen as exaggerated line on OP image at this interface of the fatty and nonfatty portions at the fracture site (Figure 5.).

This may explain why the sensitivity of OP images was higher than that of WO images, FO images, and IP images ($p < 0.05$). Based on the fact that an india ink artifact is also observed at interface of the metastatic mass with fatty marrow because neoplastic areas tend to replace or displace fatty marrow components of

bone, resulting in reduced fat and increased water content, our study did not regard the india ink artifact present at the interface of the metastatic mass with fatty marrow as fracture line.



Figure 5. Acute benign vertebral compression fractures of T10 vertebral body in a 23-year old man with Hodgkin's disease. Fracture line (arrow) was noted only on sagittal T2Weighted OP image (d) (TR/TE, 2500/100) as opposed to WO image (a), FO image (b), and IP image (c) which did not show fracture line. The faint shadow of the basivertebral vein (double arrow) were excluded from the fracture line.

Recently, Park et al reported a case of small nondisplaced chip fracture at the lateral talar dome that was well delineated only with the aid of an india ink artifact after using T2-weighted opposed-phase imaging from turbo spin-echo two-point modified Dixon ankle MRI.⁶ The full delineation of the fracture line was not possible in other sequences.⁶ These results have motivated our research and are consistent with our findings that the sensitivity of OP images to detect fracture line is higher than that of WO images, FO images, and IP images.

Also, Wohlgemuth et al mentioned the importance of FO sequence for better depicting the fracture line compared with WO or IP sequences because of its

similarity to T1-weighted image¹⁴ Though they did not compare the OP sequence, it is in line with our study where specificity of FO images was higher than that of WO images, IP images, and OP images ($p < 0.0001$). FO images provide a unique opportunity for lesion detection, as marrow signal largely emanates from fat, and lesions that replace high marrow signal are highly conspicuous against a normal background.¹³ In the absence of any bone marrow edema, a fracture line can clearly be depicted in the FO images as a black line in the very hyperintense bone marrow (Figure 1-b.).¹⁴ On the other hand, in case of the almost complete collapse of vertebral body, it is hard to detect fracture line because bone marrow edema completely replace or displace fatty marrow, resulting in diffuse hypointense marrow signal. Figure 6. shows diffuse hypointensity on FO images which makes radiologist hard to detect fracture line.

Fracture lines were visualized in WO images as subtle hypointense lines in the very hyperintense bone marrow edema,¹⁴ but there was no statistically significant diagnostic performance in the WO images.

The fact that the character of FO image is similar to a T1-weighted image and IP image is similar to a T2-weighted image would make our research meaningful. First, it would make acquisition of an additional T1-weighted sequence for visualization of the fracture line unnecessary.¹⁴ Saving acquisition time is worth to be used for practical setting. Moreover, our study demonstrates that mDixon MRI sequences, more precisely OP and FO images, are superior to the conventional MRI image in detecting fracture line. This explains why mDixon MRI could be used as a standalone technique, and might not typically be evaluated in conjunction with spin-echo T1-weighted sequences.

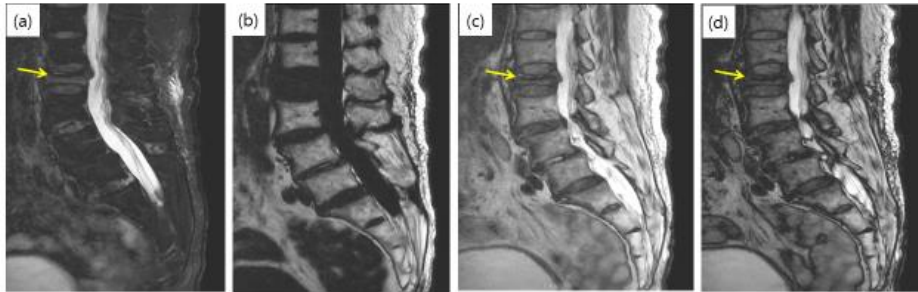


Figure 6. Successful detection of intravertebral fracture line using modified Dixon MRI technique except for FO image. Diffuse hypointense marrow signal in a benign vertebral compression fracture on FO image. Fat only image demonstrates a benign vertebral compression fracture of L2 vertebral body in a 83-year old woman without known history of malignancy. Sagittal T2-weighted water only image (a), in phase image (c), opposed phase image (d) (repetition time/echo time, 3000/80) show signal loss fracture line at fracture site when compared with fat only image (b), which did not show fracture line. Sharp black line at fat-water interfaces is recognized on opposed image (d) by observers, indicating india ink artifact.

The current study had some limitations. First, our study included a large number of benign VCFs in patients with history of known malignancy. Diffuse tumor infiltration under the malignant diseases would completely replace the normal fat marrow signal. Thereby, diffuse hypointensity on FO images interferes radiologist with detecting fracture line on FO images. Second, it is not clear whether the PET-CT within 5months from the time of mDixon MRI examination we used to differentiate between benign VCFs and malignant VCFs is always accurate. Third, the evaluation of multiple lesions in one patient can cause a clustering effect. Fourth, our study assumed that fracture line is only observed in the case of benign VCFs, however, fracture line could be seen in the case of pathologic VCFs (93% of acute osteoporotic fractures vs

44% of metastatic fractures, $p < .001$)⁵.

V. CONCLUSION

OP images showed significantly higher sensitivity for detecting fracture lines than WO images, FO images, and IP images. FO images showed significantly higher specificity for detecting fracture lines than WO images, IP images, and OP images. Therefore, mDixon MRI may be a helpful option in patients to discriminate benign and malignant VCFs focusing on intravertebral fracture line.

REFERENCES

1. Bley TA, Wieben O, Francois CJ, Brittain JH, Reeder SB. Fat and water magnetic resonance imaging. *J Magn Reson Imaging* 2010;31:4-18.
2. Eggers H, Brendel B, Duijndam A, Herigault G. Dual-echo Dixon imaging with flexible choice of echo times. *Magn Reson Med* 2011;65:96-107.
3. Earls JP, Krinsky GA. Abdominal and pelvic applications of opposed-phase MR imaging. *AJR Am J Roentgenol* 1997;169:1071-7.
4. Hashemi RH, Bradley WG, Lisanti CJ. Artifacts in MRI. In: Hashemi RH, Bradley WG, Lisanti CJ, editors. *MRI : the Basics*. 3rd ed. Philadelphia: Wolters Kluwer Health; 2012. p.185-214.
5. Israel GM, Hindman N, Hecht E, Krinsky G. The use of opposed-phase chemical shift MRI in the diagnosis of renal angiomyolipomas. *AJR Am J Roentgenol* 2005;184:1868-72.
6. Park EH, Lee KB. Usefulness of black boundary artifact on opposed-phase imaging from turbo spin-echo two-point mDixon MRI for delineation of an arthroscopically confirmed small fracture of the lateral talar dome: A case report. *Medicine (Baltimore)* 2017;96:e9497.
7. Jung HS, Jee WH, McCauley TR, Ha KY, Choi KH. Discrimination of metastatic from acute osteoporotic compression spinal fractures with MR imaging. *Radiographics* 2003;23:179-87.
8. Lee SH, Lee YH, Hahn S, Suh JS. Fat fraction estimation of morphologically normal lumbar vertebrae using the two-point mDixon turbo spin-echo MRI with flexible echo times and multipeak spectral model of fat: Comparison between cancer and non-cancer patients. *Magn Reson Imaging* 2016;34:1114-20.
9. Erly WK, Oh ES, Outwater EK. The utility of in-phase/opposed-phase imaging in differentiating malignancy from acute benign compression fractures of the spine. *AJNR Am J Neuroradiol* 2006;27:1183-8.

10. Buxton RB, Wismer GL, Brady TJ, Rosen BR. Quantitative proton chemical-shift imaging. *Magn Reson Med* 1986;3:881-900.
11. Baur A, Stabler A, Huber A, Reiser M. Diffusion-weighted magnetic resonance imaging of spinal bone marrow. *Semin Musculoskelet Radiol* 2001;5:35-42.
12. Swartz PG, Roberts CC. Radiological reasoning: bone marrow changes on MRI. *AJR Am J Roentgenol* 2009;193:S1-4, Quiz S5-9.
13. Zhadanov SI, Doshi AH, Pawha PS, Corcuera-Solano I, Tanenbaum LN. Contrast-Enhanced Dixon Fat-Water Separation Imaging of the Spine: Added Value of Fat, In-Phase and Opposed-Phase Imaging in Marrow Lesion Detection. *J Comput Assist Tomogr* 2016;40:985-90.
14. Wohlgemuth WA, Roemer FW, Bohndorf K. Short tau inversion recovery and three-point Dixon water-fat separation sequences in acute traumatic bone fractures at open 0.35 tesla MRI. *Skeletal Radiol* 2002;31:343-8.

ABSTRACT (IN KOREAN)

논문 제목

<지도교수 서진석>

연세대학교 대학원 의학과

김보연

이 연구는 척추체 내부의 골절선으로 양성 척추 압박 골절과 악성 척추 압박 골절을 감별하는 것에 modified Dixon 자기공명영상이 진단적 역할을 하는가를 평가하는 것이다.

60명의 환자가 초기 명부에 올랐으며, 이들은 2014년 4월부터 2016년 8월까지 시상면 T2강조 two-point modified Dixon 터보스핀에코영상에서 척추압박골절을 진단받은 자였다.

제외 기준을 적용한 후 37명의 환자가 남았으며, 이들은 임상적 병력, 조직검사, 자기공명영상 검사 전후 5개월 이내의 양전자 방출 컴퓨터 단층 촬영 결과에 따라 양성 척추 압박 골절군과 악성 척추 압박 골절군으로 분류되었다.

두 명의 근골격 영상의학 전문의가 시상면 T2 강조 two-point modified Dixon 터보스핀에코영상을 판독하였으며, 척추체 내부의 골절선 유무를 독립적으로 평가하였다. 일반화된 산정 균등화 및 가중치 최소 자승법을 이용하여 water only, fat only, in phase, opposed phase 각각에서의 골절선 발견의 민감도, 특이도, 양성예측도, 음성예측도, 정확도를 산출하였으며, 관찰자 간 신뢰도는 카파 계수를 이용하여 평가하였다.

총 73개/37명의 척추 압박 골절 중 32개/14명이 양성 압박

골절이었고, 나머지 41개/23명은 악성 압박 골절이었다. *Opposed phase* 의 민감도는 *water only* 영상, *fat only* 영상, *in phase* 영상보다 통계적으로 유의하게 높았으며, *fat only* 영상의 특이도는 *water only* 영상, *in phase* 영상, *opposed phase* 영상과 비교시 통계적으로 유의하게 높았다. 관찰자 간 신뢰도는 *substantial-good* 이었다.

결론적으로, *two-point modified Dixon* 자기공명영상을 이용할 시, 기존 영상기법보다 척추체 내부의 골절선을 더 잘 발견하게 되고, 이를 통해 양성 압박 골절과 악성 압박 골절의 감별에 도움을 받을 수 있다는 것이 증명되었다.

핵심되는 말 : *modified Dixon*, 자기공명영상, 양성, 악성, 척추 압박 골절, 골절